LETTERS

Charon's size and an upper limit on its atmosphere from a stellar occultation

B. Sicardy[1,2], A. Bellucci[1], E. Gendron[1], F. Lacombe[1], S. Lacour[1], J. Lecacheux[1], E. Lellouch[1], S. Renner[1], S. Pau[1], F. Roques[1], T. Widemann[1], F. Colas[3], F. Vachier[3], R. Vieira Martins[3,15], N. Ageorges[4], O. Hainaut[4], O. Marco[4], W. Beisker[5], E. Hummel[5], C. Feinstein[6], H. Levato[7], A. Maury[8], E. Frappa[9], B. Gaillard[10], M. Lavayssière[10], M. Di Sora[11], F. Mallia[11], G. Masi[11,12], R. Behrend[13], F. Carrier[13], O. Mousis[14], P. Rousselot[14], A. Alvarez-Candal[15], D. Lazzaro[15], C. Veiga[15], A. H. Andrei[15,16], M. Assafin[16], D. N. da Silva Neto[16], C. Jacques[17], E. Pimentel[17], D. Weaver[18], J.-F. Lecampion[19], F. Doncel[20], T. Momiyama[20] & G. Tancredi[21]

Pluto and its satellite, Charon (discovered in 1978; ref. 1), appear to form a double planet, rather than a hierarchical planet/satellite couple. Charon is about half Pluto's size and about one-eighth its mass. The precise radii of Pluto and Charon have remained uncertain, leading to large uncertainties on their densities[2]. Although stellar occultations by Charon are in principle a powerful way of measuring its size, they are rare, as the satellite subtends less than 0.3 microradians (0.06 arcsec) on the sky. One occultation (in 1980) yielded a lower limit of 600 km for the satellite's radius[3], which was later refined to 601.5 km (ref. 4). Here we report observations from a multi-station stellar occultation by Charon, which we use to derive a radius, $R_C = 603.6 \pm 1.4$ km (1σ), and a density of $\rho = 1.71 \pm 0.08$ g cm^{-3}. This occultation also provides upper limits of 110 and 15 (3σ) nanobar for an atmosphere around Charon, assuming respectively a pure nitrogen or pure methane atmosphere.

Charon occulted the 15th magnitude star UCAC2 26257135 on 11 July 2005, as initially predicted by D. Herald (personal communication). Charon's occultation shadow swept South America, where some of the largest telescopes in the world were available. Table 1 provides the timing of the occultation at three stations, yielding kilometre-level accuracy on the length of the occultation segments (or 'chords') at each station, using Charon's shadow velocity. We performed circular fits to the chord extremities (the three red segments in Fig. 1), the three free parameters being the two coordinates of Charon's centre and its radius. The chord extremities were weighted according to the uncertainties in the occultation times, converted into radial uncertainties, perpendicular to Charon's limb. The best fit yields a standard radial deviation of 1.1 km, and a χ^2 value per degree of freedom of 0.85 (Table 2), indicating a satisfactory fit. The corresponding radius of Charon is $R_C = 603.6 \pm 1.4$ km (formal 1σ error), assuming that the limb is circular, that is, that there are only three free parameters to adjust.

Our data do not reveal significant departures from circularity. Although elliptical fits do improve the residuals, they also reduce the number of degrees of freedom of the fit, by adding the oblateness and ellipse orientation as free parameters. This eventually worsens the χ^2 per degree of freedom (Table 2), but also increases the formal error bar on R_C from 1.4 to 5 km. We obtain a 1σ upper limit of 8×10^{-3} for the limb oblateness, fifty times larger than the value expected for a slow 6.4-day rotator in hydrostatic equilibrium. Furthermore, local topographic features might alter our determination of R_C by a few kilometres. Larger features (height >10 km) are not expected to occur, as they should relax over geologic timescales owing to the structural weakness of methane and nitrogen ices[5]. Also, our measurements apply to Charon's shape projected in the instantaneous plane of the sky, with no access to other planes. All considered, however, the global uncertainty on R_C should be smaller than 5 km. Finally, in the presence of a tenuous atmosphere, the stellar rays would be refracted towards the Earth, resulting in a shadow slightly reduced compared to Charon's body (see below).

Our result comes after two decades of extensive discussions on Charon's radius[6]. The values derived from the mutual events—occultations and eclipses of Pluto by Charon and vice versa—observed in the 1980s range from $R_C = 590 \pm 5$ km, to 592 ± 13 km, 611 ± 30 km and 627 ± 21 km (refs 7, 8, 9 and 10, respectively, 1σ error bars), assuming a semimajor axis of 19,599 km for Charon. They are thus all within 1.2σ of our value (except for the first value, at 2.7σ). Their differences mainly reflect the use of different data sets, and in some cases, of different modelling (albedo features or limb darkening).

A recent, improved orbit for Charon includes observations with the Hubble Space Telescope[2,11,12], besides older measurements made since 1978. The physical parameters used for this orbit are, among others (R. A. Jacobson, personal communication): total mass of the system $M = (1.463 \pm 0.0033) \times 10^{22}$ kg, mass ratio Charon/Pluto $f = 0.121 \pm 0.006$, semimajor axis $a = 19{,}599.0 \pm 15$ km. This provides Charon's mass $m_C = (1.58 \pm 0.07) \times 10^{21}$ kg, where most of the error bar comes from the uncertainty on f. Combining this mass with our value of R_C yields Charon's density $\rho_C = 1.71 \pm 0.08$ g cm^{-3}, where most of the error bar comes from the uncertainty on Charon's mass, as its volume is now accurately

[1]Observatoire de Paris, LESIA, 92195 Meudon cedex, France. [2]Université Pierre et Marie Curie, 75252 Paris cedex 5, France. [3]Observatoire de Paris, IMCCE, 75014 Paris, France. [4]European Southern Observatory, Alonso de Córdova 3107, Casilla 19001, Santiago 19, Chile. [5]International Occultation Timing Association, European Section, 30459 Hannover, Germany. [6]Facultad de Ciencias Astronómicas y Geofísicas, Observatorio Astronómico & Instituto de Astrofísica de La Plata, CONICET, Paseo del Bosque 1900 La Plata, Argentina. [7]Complejo Astronómico, El Leoncito, CP J5402DSP, San Juan, Argentina. [8]Gene Shoemaker Observatory, Casilla 21, San Pedro de Atacama, Chile. [9]Planétarium de Saint-Etienne, 42100 Saint-Etienne. France. [10]Association des Utilisateurs de Détecteurs Electroniques (AUDE), France, c/o F. Colas, 45, Av. Reille, 75014 Paris, France. [11]Campo Catino Austral Observatory, Casilla 21, San Pedro de Atacama, Chile. [12]Università di Tor Vergata di Roma, Via della Ricerca Scientifica n.1, 00133, Rome, Italy. [13]Observatoire de Genève, CH-1290 Sauverny, Switzerland. [14]Observatoire de Besançon, BP1615, 25010 Besançon cedex, France. [15]Observatório Nacional, 20921-400, Rio de Janeiro, Brazil. [16]Observatório do Valongo/UFRJ, CEP 20080-090, Rio de Janeiro, Brazil. [17]Observatório CEAMIG-REA, CEP 31545-120, Belo Horizonte, MG, Brazil. [18]Observatório Astronômico Christus, Universidade de Fortaleza, rua João Carvalho, 630, CEP 60140-140 Fortaleza, Brazil. [19]Observatoire Aquitain des Sciences de l'Univers, 33270 Floirac, France. [20]Observatorio Astronómico, Universidad Nacional de Asunción 2169, Paraguay. [21]Observatorio Astronómico Los Molinos, Facultad de Ciencias, 11400 Montevideo, Uruguay.

Table 1 | Circumstances of observations for the 11 July 2005 Charon occultation

Site*	Telescope, cycle time, effective wavelength	Latitude, longitude, altitude	Disappearance†, re-appearance† (h:min:s, UT, 11 July 2005)	Shadow velocity (km s^{-1})
San Pedro de Atacama	'Campo Catino Austral Telescope'	68° 10′ 48.2″ W,	03:36:20.98 ± 0.18,	21.347
	(0.5 m), 0.716 s, 0.65 μm	22° 57′ 08.4″ S, 2,410 m	03:36:28.30 ± 0.30	21.347
Paranal	'Yepun' VLT	70° 24′ 07.9″ W,	03:36:18.09 ± 0.04,	21.345
	(8.2 m), 0.2 s, 2.2 μm	24° 37′ 31.0″ S, 2,635 m	03:36:55.40 ± 0.05	21.345
El Leoncito	'Jorge Sahade Telescope'	69° 17′ 44.9″ W,	03:36:15.03 ± 0.16,	21.317
	(2.15 m), 1 s, 0.7 μm	31° 47′ 55.6″ S, 2,492 m	03:37:02.98 ± 0.08	21.317

*We attempted observations of the Charon occultation from Argentina, Bolivia, Brazil, Chile, Paraguay and Uruguay. Owing to weather conditions or technical problems, not all the stations recorded the event. The present paper is based on data gathered at San Pedro de Atacama (Chile), at Cerro Paranal (Chile) with the Very Large Telescope (VLT) of the European Southern Observatory, and at El Leoncito (Argentina), listed here. Whereas observations at both San Pedro and El Leoncito were made with fast broadband visible CCD, the Paranal observations were achieved with the NACO adaptive optics camera using a K_S band filter (2.2 μm). In the latter case, we were able to resolve the Pluto/Charon pair, with the two objects separated by 0.89 arcsec during the occultation. Beyond the three stations listed above, the occultation was also observed from La Silla (Chile) with the 1.2-m swiss telescope in drift scan mode, but at irregular speed, making the use of the light curve impossible in this paper. We furthermore obtained data from Asunción (Paraguay) with a 0.45-m telescope and a broadband CCD detector. Owing to their large cycle time (7 s), however, these data are not included in this analysis. Images were finally acquired at the CEAMIG-REA 0.3-m telescope in Belo Horizonte (Brazil), under partly cloudy conditions and with poor signal-to-noise ratio, making this data set unusable for the present analysis.
†The disappearance and reappearance times are obtained by fitting an abrupt edge shadow to the light curves, after convolving the shadow by Fresnel diffraction, stellar diameter (0.42 km projected at Charon) and finite integration time of the instrument. The error bars on the timings are 1σ level (68.3% confidence level) provided by those fits.

determined. This is true as long as the uncertainty on R_C remains smaller than 10 km, a safe margin, as discussed earlier.

Comparison with Pluto's density is problematical, however, as the planet radius is not so accurately determined. Owing to refraction by Pluto's atmosphere, occultation determination of Pluto's radius, R_P, still depends on atmospheric models[13]. An upper limit of $R_P = 1{,}195 \pm 5$ km is given by occultations[14], while a lower limit of $R_P = 1{,}151 \pm 6$ km is provided by mutual events[6]. Combining these results with Pluto's mass, derived from the quantities above, yields Pluto's density in the range 1.8–2.1 g cm^{-3} (ref. 2), where most of the uncertainty now comes from Pluto's radius R_P, not from its mass. However, our results tighten the difference between Pluto's density and Charon's, as the latter was previously estimated[2] to lie in the interval 1.4–1.8 g cm^{-3}.

These ranges for Pluto's and Charon's densities are in good agreement with current structural models[15], which produce baseline densities of 1.85 g cm^{-3} and 1.75 g cm^{-3} for Pluto and Charon, respectively. They indicate a slightly higher rock versus ice fraction on Pluto (0.65) than on Charon (0.55–0.60). Our improved density for Charon, however, cannot distinguish differentiated and undifferentiated states of the satellite. In the framework of the giant impact model for the origin of Pluto and Charon, similar densities for the two bodies favour the scenario in which Charon is formed intact, as opposed to being accreted from a disk orbiting Pluto[16].

Note that there is now a possibility of improving these numbers by re-analysing the mutual events of the 1980s, using the value of Charon's radius derived here, plus the improved orbital parameters quoted above, in order to get a more accurate value for R_P. This

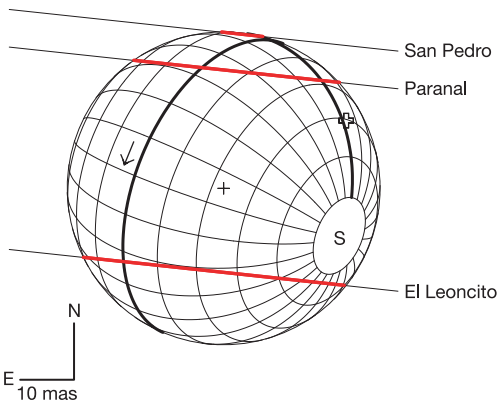

Figure 1 | Measuring Charon's radius. Charon's aspect on 11 July 2005, with celestial north up and east left, using the values in Table 2. The scale in milli-arcsec (mas) is shown, with one mas corresponding to 21.809 km projected at Charon. The thicker meridian is the origin of longitudes on Charon, that is, the meridian always facing Pluto, as the satellite is locked in a synchronous orbit. The thicker parallel is the equator. Charon's south pole (S) follows the IAU definition, the arrow indicating the satellite rotation. The star trajectories relative to Charon, as observed from San Pedro, Paranal and El Leoncito, are shown as black lines, the red parts corresponding to the segments where the star was occulted by Charon. A circular fit to these chords yields a radius of 603.6 ± 1.4 km (1σ) for Charon. The thick cross marks the expected location of Charon's centre, using the DE413/PLU013 Charon ephemeris, and the ICRF/J2000 star position given in Table 2. The thin cross is the centre of the circular fit, showing that Charon's DE413/PLU01 position must be corrected by $\Delta\alpha\cos(\delta) = +22 \pm 11$ mas (towards the east) and $\Delta(\delta) = -12 \pm 11$ mas (towards the south), where the error bars come from the uncertainties on the star position. This offset is mostly attributable to an error on Pluto's barycentric DE413 ephemeris, rather than to an offset of Charon's PLU013 ephemeris around Pluto. In fact, adaptive optics images taken with the NACO/VLT camera at Paranal show that Charon is at only 4 mas from its calculated position relative to Pluto, an effect that could be entirely due to photocentre displacements caused by albedo features on Pluto and/or Charon.

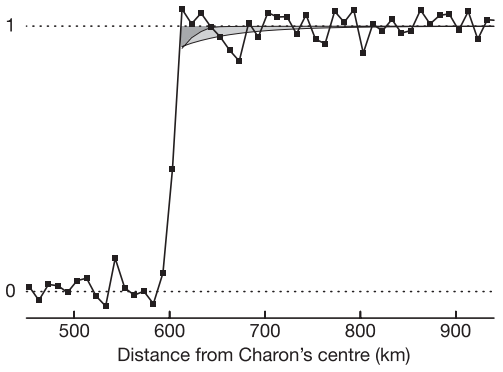

Figure 2 | Limit on Charon's atmosphere. The stellar flux from Leoncito and Paranal before and after the occultation has been rebinned in intervals of 10 km in radial distance from Charon's centre. The two data sets have then been averaged with weights taking into account their respective noise levels, resulting in the light curve shown here (black squares connected by a line). The values have been normalized between zero (no stellar flux) and unity (full stellar flux), as indicated by the dotted lines. Two examples of atmospheric models are shown superimposed on the data. Light grey model: expected drop of signal with an isothermal N_2 atmosphere at $T = 56$ K, with a pressure of $p_s = 110$ nbar at Charon's surface. Dark grey model: effect of a CH_4 atmosphere with $T = 56$ K and $p_s = 15$ nbar at the surface, with T increasing to 100 K near 20 km above the surface, thus mimicking Pluto's atmosphere temperature profile. These models illustrate upper limits of detection (at 3σ level) that we can obtain on a putative atmosphere for Charon.

Table 2 | Fits to the occultation chords

Site	f* (km)	g* (km)	Latitude† of suboccultation point (deg.)	Radial residual (km)		
				Circular fit, $\epsilon = 0$ fixed	Elliptical fit, P fixed	Elliptical fit, P free
San Pedro, disappearance	+327.1	+325.0	06.9 N	+0.26	+0.40	+0.31
San Pedro, re-appearance	+482.6	+341.6	19.1 N	−0.84	−0.75	−0.92
Paranal, disappearance	+28.7	+147.6	20.5 S	−0.14	−0.22	−0.08
Paranal, re-appearance	+820.6	+232.5	44.2 N	+0.28	+0.07	+0.11
El Leoncito, disappearance	−2.8	−636.7	52.7 S	+2.45	+1.93	+0.26
El Leoncito, re-appearance	+1,013.5	−527.6	33.2 N	−0.60	−0.25	−0.07
Free parameters				**Best-fit values**		
Charon's radius, R_C (km)				603.6	603.1	603.4
Offset‡ in right ascension, f_c (km)				472.7	472.4	+471.9
Offset‡ in declination, g_c (km)				−261.0	−260.8	+261.8
Oblateness, ϵ				0, fixed	-1.5×10^{-3}	-2×10^{-3}
North pole position angle, P (deg.)				67.6, fixed	67.6, fixed	+33.3
χ^2 per degree of freedom§				0.85	1.10	1.67

*The timings of Table 1 provide the star position relative to Charon's expected centre, using the DE413/PLU013 Charon ephemeris (http://ssd.jpl.nasa.gov). This position is projected in the plane of the sky, in km, where f is the relative position in right ascension, positive if the star is east of Charon's centre, and g is the relative position in declination, positive if the star is north of Charon's centre. We used the following ICRF/J2000 star position: $\alpha = 17\,\mathrm{h}\,28\,\mathrm{min}\,55.0167\,\mathrm{s}$ and $\delta = -15°\,00'\,54.726''$, with typical uncertainties of 11 mas, measured at the 60-cm reflector of Pico dos Dias (Laboratório Nacional de Astrofísica, Brazil), and at the meridian refractor of Bordeaux Observatory (France).

†The latitudes of the suboccultation points on Charon are derived using a north pole position angle of $P = 67.6°$ with respect to the J2000 celestial north, and a sub-Earth latitude of $B = -34.2°$.

‡This offset is the position of Charon's centre obtained from the fit (thin cross in Fig. 1), relative to Charon's centre expected from the adopted star position and the DE413/PLU013 ephemeris (thick cross in Fig. 1).

§The number of degrees of freedom is the number of data points (here $N = 6$) minus the number of free parameters: $M = 3$, $M = 4$ or $M = 5$, depending on whether the fit is circular, elliptical with P fixed, or elliptical with P free, respectively. The quantity minimized in the fits is $\chi^2 = \sum_1^N (r_{i,\mathrm{obs}} - r_{i,\mathrm{cal}})^2/\sigma_i^2$, where $r_{i,\mathrm{obs}}$ (resp. $r_{i,\mathrm{cal}}$) is the distance of the observed (resp. calculated) ith point to the shadow centre, and σ_i is the 1σ uncertainty on $r_{i,\mathrm{obs}}$.

would have important consequences for better constraining not only Pluto's density, but also the Pluto atmosphere models, through a reassessment of occultation observations.

Our data also set an upper limit for a putative atmosphere for Charon. By combining the stellar fluxes observed at the Paranal and El Leoncito observatories, we derive a synthetic light curve, as shown in Fig. 2. The effect of an atmosphere depends on the surface pressure, the nature of the gas and the temperature profile. We assumed two cases. One is that of an isothermal nitrogen (N_2) atmosphere at $T_s = 56$ K, the recently estimated mean dayside Charon surface temperature[17]. The other is a pure methane (CH_4) atmosphere, with a temperature increasing from 56 K at the surface to 100 K above 20 km, due to solar heating, as is the case for Pluto's atmosphere[14]. The two cases indicate upper limits of 110 and 15 nbar (3σ), respectively, with corresponding upper limits of 4.1 and 1.3 cm amagat for the vertical column densities. Limits obtained from the 1980 Charon stellar occultation were about two and ten times larger for N_2 and CH_4, respectively[4]. Note that in the limiting cases presented here, refraction of stellar rays by the atmosphere would cause a reduction of Charon's shadow radius by about 10 km, when compared to the actual radius, R_C. Consequently, if an atmosphere is detected at those levels in the future, such effects should be considered when deriving R_C.

The very low upper limit for an atmosphere around Charon is not surprising, given estimates of escape rates[14]. The upper limit we derive for a pure methane atmosphere is also consistent with the absence of a CH_4 ice signature in its near-infrared spectrum[18]. In fact, a 15 nbar CH_4 atmosphere is in equilibrium with CH_4 ice at 41 K, much less than the 56 K quoted above. Methane ice could still be present in restricted, colder, regions of the surface. For N_2, a 110 nbar atmosphere would imply an even lower equilibrium temperature ($T < 31$ K), requiring that N_2 ice be confined at best to high northern latitudes and/or to permanently shadowed regions of the satellite. The same is true for other candidates, like CO, which would require temperatures as low as 35 K.

Received 2 September; accepted 17 October 2005.

1. Christy, J. W. & Harrington, R. S. The satellite of Pluto. *Astron. J.* **83,** 1005–1008 (1978).
2. Olkin, C. B., Wasserman, L. H. & Franz, O. G. The mass ratio of Charon to Pluto from Hubble Space telescope astrometry with the fine guidance sensors. *Icarus* **164,** 254–259 (2003).
3. Walker, A. R. An occultation by Charon. *Mon. Not. R. Astron. Soc.* **192,** 47P–50P (1980).
4. Elliot, J. L. & Young, L. A. Limits on the radius and a possible atmosphere of Charon from its 1980 stellar occultation. *Icarus* **89,** 244–254 (1991).
5. Stern, S. A. The Pluto-Charon system. *Annu. Rev. Astron. Astrophys.* **30,** 185–233 (1992).
6. Tholen, D. J. & Buie, M. W. in *Pluto and Charon* (eds Stern, S. A. & Tholen, D. J.) 193–219 (Univ. Arizona Press, Tucson, 1997).
7. Reinsch, K., Burwitz, V. & Festou, M. C. Albedo maps of Pluto and improved physical parameters of the Pluto-Charon system. *Icarus* **108,** 209–218 (1994).
8. Tholen, D. J. & Buie, M. W. Further analysis of the Pluto-Charon mutual event observations. *Bull. Am. Astron. Soc.* **22,** 1129 (1990).
9. Buratti, B. J. *et al.* Modeling Pluto-Charon mutual events. II. CCD observations with the 60 in. telescope at Palomar Mountain. *Astron. J.* **110,** 1405–1419 (1995).
10. Young, E. F. & Binzel, R. P. A new determination of radii and limb parameters for Pluto and Charon from mutual events lightcurves. *Icarus* **108,** 219–224 (1994).
11. Null, G. W. & Owen, W. M. Jr Charon/Pluto mass ratio obtained with *HST* CCD observations in 1991 and 1993. *Astron. J.* **111,** 1368–1381 (1996).
12. Tholen, D. J. & Buie, M. W. The orbit of Charon. I. New Hubble Space Telescope observations. *Icarus* **125,** 245–260 (1997).
13. Stansberry, J. A., Lunine, J. I., Hubbard, W. B., Yelle, R. V. & Hunten, D. M. Mirages and the nature of Pluto's atmosphere. *Icarus* **111,** 503–513 (1994).
14. Yelle, R. V. & Elliot, J. L. in *Pluto and Charon* (eds Stern, S. A. & Tholen, D. J.) 347–390 (Univ. Arizona Press, Tucson, 1997).
15. McKinnon, W. B., Simonelli, S. P. & Schubert, G. in *Pluto and Charon* (eds Stern, S. A. & Tholen, D. J.) 295–343 (Univ. Arizona Press, Tucson, 1997).
16. Canup, R. M. A giant impact origin of Pluto-Charon. *Science* **307,** 546–550 (2005).
17. Gurwell, M. A. & Butler, B. J. Sub-arcsec scale imaging of the Pluto/Charon binary system at 1.4 mm. *Bull. Am. Astron. Soc.* **37,** 743 (2005).
18. Dumas, C., Terrile, R. J., Brown, R. H., Schneider, G. & Smith, B. A. Hubble Space Telescope NICMOS spectroscopy of Charon's leading and trailing hemispheres. *Astron. J.* **121,** 1163–1170 (2001).

Acknowledgements We thank the Conseil Scientifique of the Paris Observatory and the Programme National de Planétologie for supporting part of the observations of this event in South America.

Author Information Reprints and permissions information is available at npg.nature.com/reprintsandpermissions. The authors declare no competing financial interests. Correspondence and requests for materials should be addressed to B.S. (bruno.sicardy@obspm.fr).